Water Research 194 (2021) 116933

Contents lists available at ScienceDirect

Water Research

journal homepage: www.elsevier.com/locate/watres

# The impacts of reservoirs on the sources and transport of riverine organic carbon in the karst area: A multi-tracer study

Yuanbi Yi[a], Jun Zhong[a], Hongyan Bao[b,*], Khan M.G. Mostofa[a,c], Sheng Xu[a], Hua-Yun Xiao[a,d], Si-Liang Li[a,c,*]

[a] Institute of Surface-Earth System Science, School of Earth System Science, Tianjin University, Tianjin 300072, China
[b] State Key Laboratory of Marine Environmental Science, College of Ocean and Earth Sciences, Xiamen University, Xiamen 361102, China
[c] State Key laboratory of Hydraulic Engineering Simulation and Safety, Tianjin University, Tianjin 300072, China
[d] State Key Laboratory of Environmental Geochemistry, Institute of Geochemistry, Chinese Academy of Sciences, Guiyang 550002, China

ARTICLE INFO

*Article history:*
Received 29 November 2020
Revised 10 February 2021
Accepted 11 February 2021
Available online 14 February 2021

*Keywords:*
Reservoir
Biological carbon pump
Dissolved organic matter
Fluorescence
Radiocarbon

ABSTRACT

Reservoirs have been constructed as clean energy sources in recent decades with various environmental impacts. Karst rivers typically exhibit high dissolved inorganic carbon (DIC) concentrations, whether and how reservoirs affect carbon cycling, especially organic carbon (OC)-related biogeochemical processes in karst rivers, are unclear. To fill this knowledge gap, multiple tracer methods (including fluorescence excitation-emission matrix (EEM), ultraviolet (UV) absorption, and stable carbon ($\delta^{13}C$) and radiocarbon ($\Delta^{14}C$) isotopes) were utilized to track composition and property changes of both particulate OC (POC) and dissolved OC (DOC) along river-transition-reservoir transects in the Southwest China karst area. The changes in chemical properties indicated that from the river to the reservoir, terrestrial POC is largely replaced by phytoplankton-derived OC, while gradual coloured dissolved organic matter (CDOM) removal and addition of phytoplankton-derived OC to the DOC pool occurred as water flowed to the reservoir. Higher primary production in the transition area than that in the reservoir area was observed, which may be caused by nutrient released from suspended particles. Within the reservoir, the production surpassed degradation in the upper 5 m, resulting in a net DIC transformation into DOC and POC and terrestrial DOM degradation. The primary production was then gradually weakened and microbial degradation became more important down the profile. It is estimated that ~3.1–6.3 mg $L^{-1}$ (~15.5–31.5 mg-C $m^{-2}$ (~10–21%)) DIC was integrated into the OC pool through the biological carbon pump (BCP) process in the upper 5 m in the transition and reservoir areas. Our results emphasize the reservoir impact on riverine OC transport, and due to their characteristics, karst areas exhibit a higher BCP potential which is sensitive to human activities (more nutrient are provided) than non-karst areas.



## 1. Introduction

Rivers comprise the major link between the land and ocean, transporting up to 260 Tg $yr^{-1}$ of dissolved organic carbon (DOC) and approximately 200 Tg $yr^{-1}$ of particulate organic carbon (POC) to the ocean (Hedges, 1992; Raymond and Spencer, 2015). However, due to the pressure exerted by human activities on rivers, only 37% of the rivers worldwide remain free-flowing rivers (Best, 2019; Grill et al., 2019). Approximately 60 Tg of organic carbon (OC) is buried globally in inland reservoirs each year, accounting for approximately 40% of the global OC burial (Mendonca et al., 2017). More than 48,000 reservoirs with a depth greater than 15 m have been established globally since 1980 (Dams, 2000). With increasing number of reservoirs, the environmental problems caused by reservoirs become increasingly prominent (Maavara et al., 2017; Wang, 2020). For example, a reservoir may change the light conditions and hydraulic retention time of a river and may increase the retention of nutrients and the burial of sediments, resulting in different degrees of change in the transport and transformation of organic matter (OM) over natural river systems (Matzinger et al., 2007). However, systematic research on how reservoirs alter riverine OC cycling remains lacking.

Dissolved OM (DOM) plays an important role in all biological and abiotic processes in aquatic ecosystems (Hansen et al., 2016; Yang et al., 2014). DOM may be affected by many processes, whereby photodegradation and biodegradation are among

* Corresponding authors.
*E-mail addresses:* baohy@xmu.edu.cn (H. Bao), siliang.li@tju.edu.cn (S.-L. Li).

https://doi.org/10.1016/j.watres.2021.116933
0043-1354/

the two main processes in inland water bodies (Dittmar, 2015; Hansen et al., 2016; Raymond and Spencer, 2015). Photodegradation of DOM produces active nitrogen (N) (Bushaw et al., 1996; Teeling et al., 2012), which is beneficial to the growth of phytoplankton in the aquatic environment (Teeling et al., 2012). Moreover, during biodegradation, refractory DOM is produced, which then forms a potential carbon sink after burial in sediments (Jiao et al., 2010). Therefore, it is particularly important to investigate the sources and transport and transformation processes of DOM.

Natural DOM is a complex mixture composed of tens of thousands of different molecules (Dittmar, 2015). To better understand the transport and transformation of DOM in river systems, multiple methods are required. Ultraviolet (UV) absorption and the fluorescence excitation-emission matrix (EEM) technique are simple and efficient methods that have been widely applied to characterize and quantify the composition of DOM in aquatic environments (Derrien et al., 2019; Holland et al., 2018), while the (stable and radioactive) isotopes of OC effectively track the sources and transformations in water environments (Raymond and Bauer, 2001a). Therefore, the combination of the optical properties and isotopic composition of OM may help to explain its biogeochemical cycle qualitatively and quantitatively and may further provide a perspective from the bulk to the molecular level.

Global karst areas account for 15% of the Earth land area (IPCC Climate, 2007), which imposes a major effect on the terrestrial C uptake and environmental quality (Liu et al., 2018; Piao et al., 2010). As a carbon sink, reservoirs play an important role in the global carbon cycle, especially the reservoirs in karst areas (Beaulieu et al., 2012; Cole et al., 2007). Since karst water bodies usually contain 6–10 times higher concentrations of dissolved inorganic carbon (DIC) than do those in non-karst areas due to weathering (Shih, 2018; Zhong et al., 2020), they provide more favourable conditions for the biological carbon pump (BCP) process. The BCP process is an important part of the OC cycle, which often occurs on the surface of water bodies, including rivers, lakes, reservoirs and oceans. The BCP process converts inorganic carbon into OC in aquatic systems and thereby affects the carbon cycle (Liu et al., 2018). Therefore, understanding the reservoir effect in karst areas is significant in a global scale in terms of carbon cycle.

China contains the largest karst area worldwide, which is mainly found in the southwest region. Due to the abundant water resources and canyon-shaped terrain, the southwest region has become an important hydropower development area with a notable reservoir effect (Wang et al., 2019). The Hongjiadu (HJD) reservoir is the first reservoir with a multi-year regulation function in the Wujiang River Basin. In addition to the reservoir effect, it is also possible to intuitively observe the change in OC from the river to the reservoir and exclude the influence of the cascade reservoir effect. Therefore, the HJD reservoir is an ideal site to study OC transport and transformation in river-reservoir systems.

Our previous investigations focused on physical conditions and bulk OC properties showed that the most intense stratification and largest differences between rivers and reservoirs occurred in summer (supplementary file; Fig. S1 and S2); therefore, we focused our study in the summer period due to the high dynamics of the water environment (Wang et al., 2019). Multiple techniques (including optical properties and (stable and radioactive) isotopes) were applied. Our objectives are 1) to characterize the changes in the sources and composition of OC in the river-reservoir continuum; 2) to quantify how the reservoir affects the transport and transform of OC; and 3) to propose a conceptual model of the effect of the reservoir on carbon cycling. Our results not only reflect the important role that reservoirs play in reservoir systems but also provide a theoretical basis to analyze the transport and transformation of OC from a systematic perspective.

## 2. Materials and methods

### 2.1. Site description

The Wujiang River is the largest tributary of the Yangtze River, in Guizhou Province, China. The Wujiang River has a total length of 1037 km with a watershed area of $87.92 \times 10^6$ km$^2$. The climate in the study region is classified as a subtropical humid monsoon climate, with an annual rainfall and mean temperature of ~1180 mm and 15 °C, respectively (Gzqx, 2018). The river is located in a karst area and features notable carbonate weathering. The depth of the HJD is 125 m, and due to its water volume regulation function, the average annual flow rate is 155 m$^3$ $s^{-1}$. The HJD reservoir exhibits the longest water retention time and highest water level in summer, and the lowest values are observed in winter (Table S1). The site has been classified to three regions (river region, transition region and reservoir region) according to the changes in the carbon chemistry, which undergoes temporal changes throughout the year.

### 2.2. Sampling and analytical methods

Surface water samples (0.5 m) along the river-reservoir transect in tributary, mainstream and a depth profile (ranging from the surface (0.5 m) to near the bottom (125 m)) were collected from the HJD reservoir in August 2018 using a Niskin water sampler (model 1010, General Oceanics, USA) (Fig. 1). The pH, Chlorophyll-a (Chl-a), water temperature (T) and dissolved oxygen saturation (DO%) were measured *in situ* with an automated multi-parameter profiler (model YSI 6600), which was calibrated on site.

The water samples were filtered through glass fiber filters (Whatman GF/F, pre-combusted at 450 °C for 4 h) immediately after sampling. The particulate matter retained on the filters were stored at -20 °C until the analyze for the concentration and isotopes of POC. The filtrate was acidified with phosphoric acid to pH = 2 and stored at 4 °C for DOC analysis, and were stored in high-density polyethylene bottles at 4 °C and tested within two days for UV and EEM analysis. For the DIC analysis, the water samples were first filtered in the field using 0.45-$\mu$m polytetrafluoroethylene syringe filters and then 2-mL samples was injected into 10-mL LABCO bottles under pre-treatment vacuum, and 1 mL phosphoric acid was added with a syringe.

#### 2.2.1. The concentration and isotope analysis of DIC, DOC and POC

The concentration of the DOC was determined on an Aurora 1030 total OC analyser (OI Analytical, USA) with duplicates (±1.5%, analytical error). In regard to the elemental and carbon isotope analysis of the particulate samples, the GF/F filters were first acidified to remove any inorganic carbon (Bao et al., 2014), and the concentration of POC and total nitrogen (TN) was tested with an elemental analyser (Euro Vector, EA3000, Italy) (±5%, analytical error). The C/N was then calculated as the weight ratio of POC to TN. The concentration of DIC was determined by titration with HCl at 0.02 mol $L^{-1}$ in the field within 12 h (Telmer and Veizer, 1999).

For the isotopes of DOC, the filtrate (5 L) were first concentrated through rotary evaporation and oxidized into $CO_2$ gas in a vacuum line system via wet oxidation (Leonard et al., 2013). The generated $CO_2$ were then divided into two parts for $\delta^{13}C$ ($\delta^{13}C_{DOC}$) and $\Delta^{14}C$ ($\Delta^{14}C_{DOC}$) analysis. The $CO_2$ partitioned for the $\delta^{13}C_{DOC}$ analysis was directly tested with a 253 Plus instrument (Thermo Fisher, ±0.1‰, analytical error), and was converted into graphite (Xu et al., 2007) and tested in an accelerator mass spectrometry (AMS) system (±3‰, analytical error) for $\Delta^{14}C_{DOC}$ at Tianjin University.

For $\delta^{13}C$ of POC ($\delta^{13}C_{POC}$), the sample after acidification was directly tested in a Flash 2000 HT device coupled with the 253 Plus instrument (Thermo Fisher, ±0.2‰, analytical error), and the

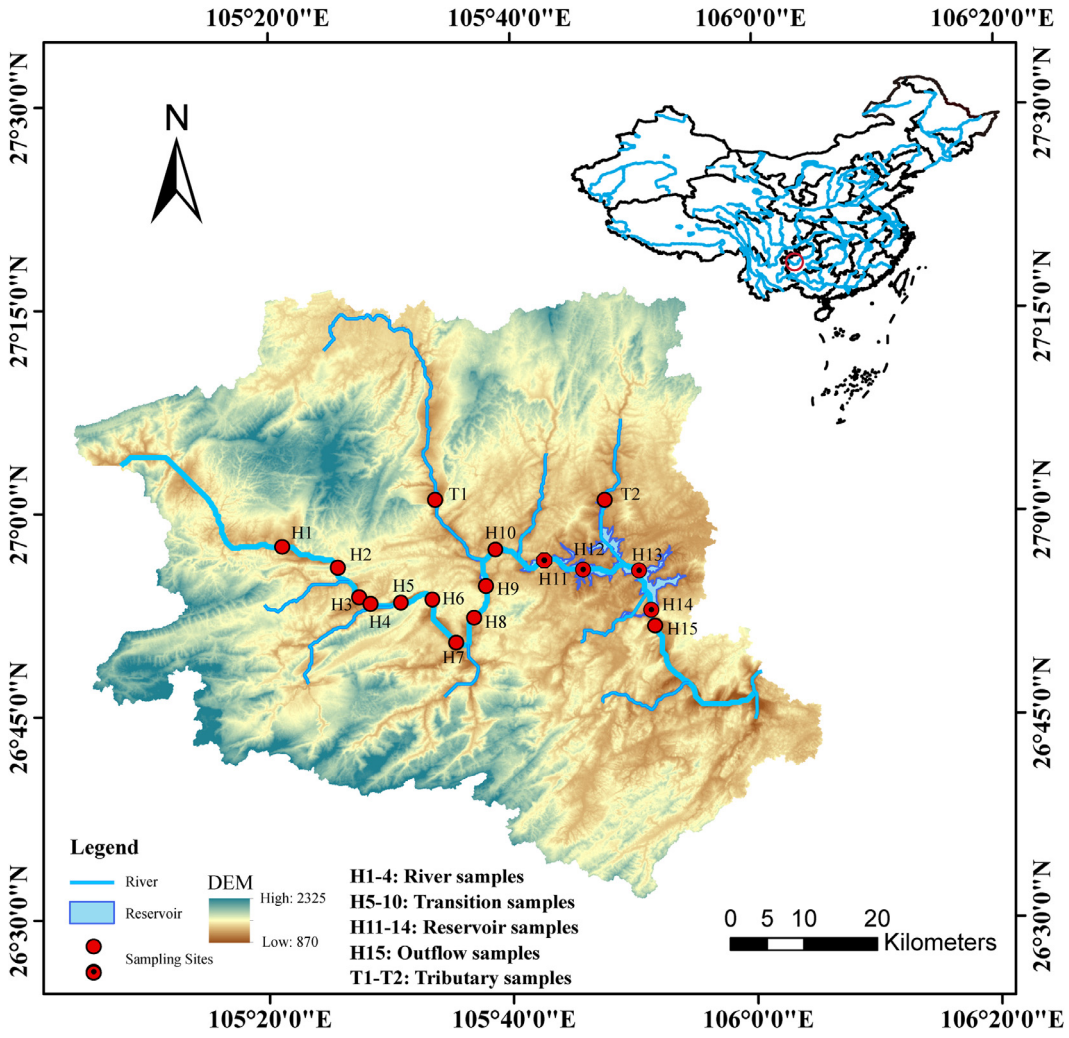


**Fig. 1.** Study area and sampling points in the river-reservoir system of the Hongjiadu (HJD) reservoir.

$\Delta^{14}C$ sample was combusted at 850 °C for 2 h under vacuum and evolved $CO_2$ was transformed into graphite and tested via AMS. The $\Delta^{14}C_{DOC}$ and $\Delta^{14}C_{POC}$ were calibrated with the $\delta^{13}C$ value of the sample (Stuiver and Polach, 1977). The $\delta^{13}C$ of DIC ($\delta^{13}C_{DIC}$) were determined with a gas bench coupled with a Delta V Plus instrument (Thermo Fisher, ±0.3‰, analytical error) as previously reported (Zhou et al., 2015).

*2.2.2. Optical properties of DOM*

A UV–visible (Vis) spectrophotometer (UV-2700, Shimadzu) was used to estimate the absorbance of the filtered water samples ($\lambda$ = 200–750 nm). Various optical parameters, including the absorption coefficient [a($\lambda$)] and specific UV absorbance at 254 nm [$SUVA_{254}$ (L $mg^{-1}$ $m^{-1}$)], were calculated (Griffin et al., 2018; Helms et al., 2008).

EEMs were tested with a fluorescence spectrophotometer (F-7000, Hitachi, Japan) using previously reported measurement procedures (Mostofa et al., 2019). The detailed procedure followed in applying PARAFAC model to EEM spectra and the validation of PARAFAC model is provided in supplementary text.

*2.3. Statistical analyses*

Pearson's correlation between the different parameters was analysed with R 4.0.2, where the ± notation represents the standard deviation if not otherwise mentioned.

## 3. Results

*3.1. Basic physical parameters*

The physical conditions from the river to the reservoir area changed significantly (Fig. 2(a)). Along the direction of water flow, the temperature (20.8–27.6 °C), pH (8.2–9.0), Chl-a (1.6–3.3 $\mu g$ $L^{-1}$) and DO% (102.2%-121.4%) all revealed clear increasing trends, while they were all the lowest at the reservoir outlet (H15), which were 16.8 °C, 7.7, 0.3 $\mu g$ $L^{-1}$ and 57.3%, respectively. The temperature profile (12.9–27.7 °C) showed a decreasing trend from the surface to the 120 m depth (Fig. 3(a)). DO%, Chl-a and pH were 14.7–121.4%, 0.1–10.3 $\mu g$ $L^{-1}$ and 7.6–8.5, respectively, which showed similar trends, both first decreased from surface to 15 m, and then gradually increased.

*3.2. The concentration of the total suspended matter (TSM), DIC, DOC and POC*

TSM, DIC and POC were 1.2–48 mg $L^{-1}$, 12.9–30.8 mg $L^{-1}$ and 0.4–1.4 mg $L^{-1}$, respectively, and all exhibited a general decreasing trend along the river-reservoir continuum (Fig. 2(b)). At the reservoir outlet, the TSM level (0.5 mg $L^{-1}$) remained low, while the DIC concentration (28.7 mg $L^{-1}$) returned to a level close to that observed at the river sites (Fig. 2(b)). DOC increased from the river (0.9±0.1 mg $L^{-1}$) to the reservoir (1.6±0.1 mg $L^{-1}$) and de-

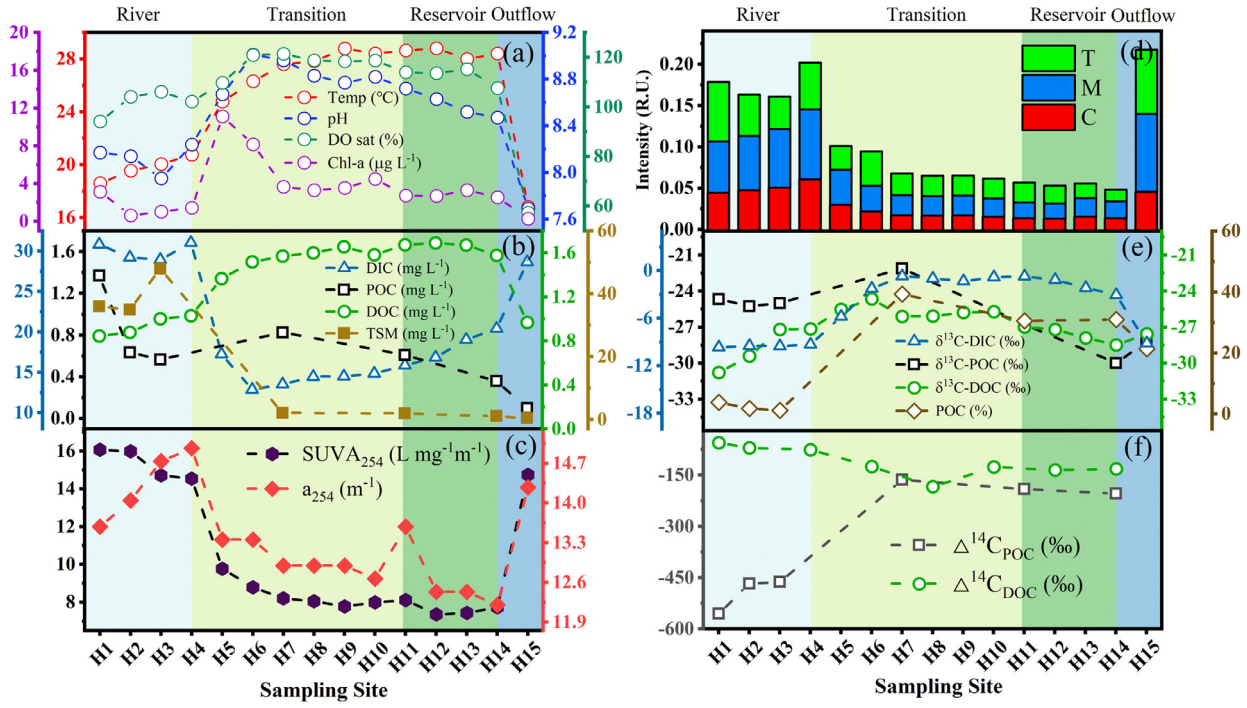


**Fig. 2.** Diagram of the changes of different parameters in the surface water along the river-to-reservoir transect: a) The temperature, pH, chlorophyll-a and dissolved oxygen; b) the concentrations of DOC, DIC, POC and TSM; c) variation of $a_{254}$ and $SUVA_{254}$; d) the variations of different FDOM components (Peak C, M and T); e) the $\delta^{13}C$ values of POC and DOC and POC%; f) changes in $\Delta^{14}C_{DOC}$ and $\Delta^{14}C_{POC}$.

creased to a concentration (1.0 mg $L^{-1}$) similar to that observed at the riverine sites at the outlet. The proportion of POC (POC%) was the lowest in the river area (2±1%) and the highest in the reservoir area (34±4%) (Fig. 2(e)). The C/N ratio of POC was high in the river area (9.3±0.8) but much lower in the transition and reservoir areas (6.0±0.2).

In the reservoir profile, TSM, DIC, POC and DOC were 0.1–1.0 mg $L^{-1}$, 20.1–30.8 mg $L^{-1}$, 0.1–0.4 mg $L^{-1}$, and 0.8–1.6 mg $L^{-1}$, respectively (Fig. 3(b)). TSM, POC and DOC all showed decreasing trends from the surface to the bottom layer, while DIC exhibited the opposite trend. The DIC and DOC concentrations from 60 to 80 m were close to those at the riverine sites.

### 3.3. The optical properties of DOM

The $a_{254}$ (indicating the content of CDOM) and $SUVA_{254}$ (indicating the aromaticity of DOM) (Griffin et al., 2018; Helms et al., 2008) values demonstrated similar decreasing trends along the river-reservoir transect (Fig. 2(c)) and were 14.34 $m^{-1}$ to 12.3 $m^{-1}$ and 15.34 L $mg^{-1}$ $m^{-1}$ to 7.59 L $mg^{-1}$ $m^{-1}$, respectively. Both parameters then increased to values similar to those observed at the riverine sites at the reservoir outlet. Three fluorescent DOM (FDOM) components were identified, including terrestrial humic-like C-type substances, autochthonous humic-like M-type substances and tryptophan-like T-type substances, in the surface samples (Fig. S3). Peaks C, M, and T showed similar trends to those of $a_{254}$ and $SUVA_{254}$ and were all significantly higher in the river area (H1-H4) and outflow area (H15) than they were in the transition and reservoir areas (H5–H14) (Fig. 2(d)).

In the reservoir, $a_{254}$ attained the highest value (14.74 $m^{-1}$) from 15–45 m and relatively low values from 0–15 m (12.74±0.22 $m^{-1}$) and 45–120 m (13.18±0.19 $m^{-1}$) (Fig. 3(c)). $SUVA_{254}$ gradually increased from the surface (7.63 L $mg^{-1}$ $m^{-1}$) to 120 m (17.26 L $mg^{-1}$ $m^{-1}$) (Fig. 3(c)) and remained relatively constant below 60 m (16.61±0.99 L $mg^{-1}$ $m^{-1}$). In the reservoir profile, all the fluorescent components were relatively low from 0–5 m (Fig. 3(d)). Peak C exhibited a slight change from 15–120 m, while peak M exhibited a much smaller change than did peak C from 15–80 m and then disappeared from 100–120 m. A new protein peak (newly released protein-like substances, namely, peak Newly) of phytoplankton origin with a strong signal (0.17±0.02) was generated from 100–120 m. Peak T was the highest from 100–120 m (0.093±0.005), followed by 15–45 m (0.055±0.005), and it was the lowest from 60–80 m (0.034±0.002).

### 3.4. The stable and radioactive isotopes of DIC, DOC and POC

The $\delta^{13}C_{DIC}$ and $\delta^{13}C_{DOC}$ was -9.5 to -2.6‰ and -28.6 to -26.8‰, respectively, and showed similar trends, with most enriched values occurring in the transition area and most depleted values occurring in the river area. The $\delta^{13}C_{POC}$ ranged from -29.5‰ to -24.7‰, which also exhibited the most enriched value (-22.1‰) in the transition area and the most depleted value in the reservoir area. The $\Delta^{14}C_{DOC}$ became increasingly depleted from the river area (-67±9‰) to the reservoir area (-140±22‰), while $\Delta^{14}C_{POC}$ became increasingly enriched from the river area (-495±43‰) to the reservoir area (-186±17‰).

In the reservoir profile, $\delta^{13}C_{DIC}$ was enriched at 0–10 m (-3.1±0.1‰) and then remained at a relatively depleted and invariable value below 15 m (-9.40.2‰) (Fig. 3(e)). $\delta^{13}C_{DOC}$ was -28.5‰ to -27.1‰, and first showed an increasing trend from 0 m to 15 m, followed by a decreased from 15 m to 80 m (-30.1‰), and gradually increased to -27.7‰ at 120 m. $\delta^{13}C_{POC}$ was -32.9‰ to -29.5‰, and exhibited almost the opposite trends to those of DOC. The $\Delta^{14}C_{DOC}$ and $\Delta^{14}C_{POC}$ also showed opposite trends in the profile (Fig. 3(f)). $\Delta^{14}C_{DOC}$ increased from 0 m (-131‰) to 120 m (-78‰), of which the most positive value occurred at 80 m (-71‰), while $\Delta^{14}C_{POC}$ decreased from 0 m (-204‰) to 120 m (-303‰), with the most negative value also observed at 80 m (-330‰).

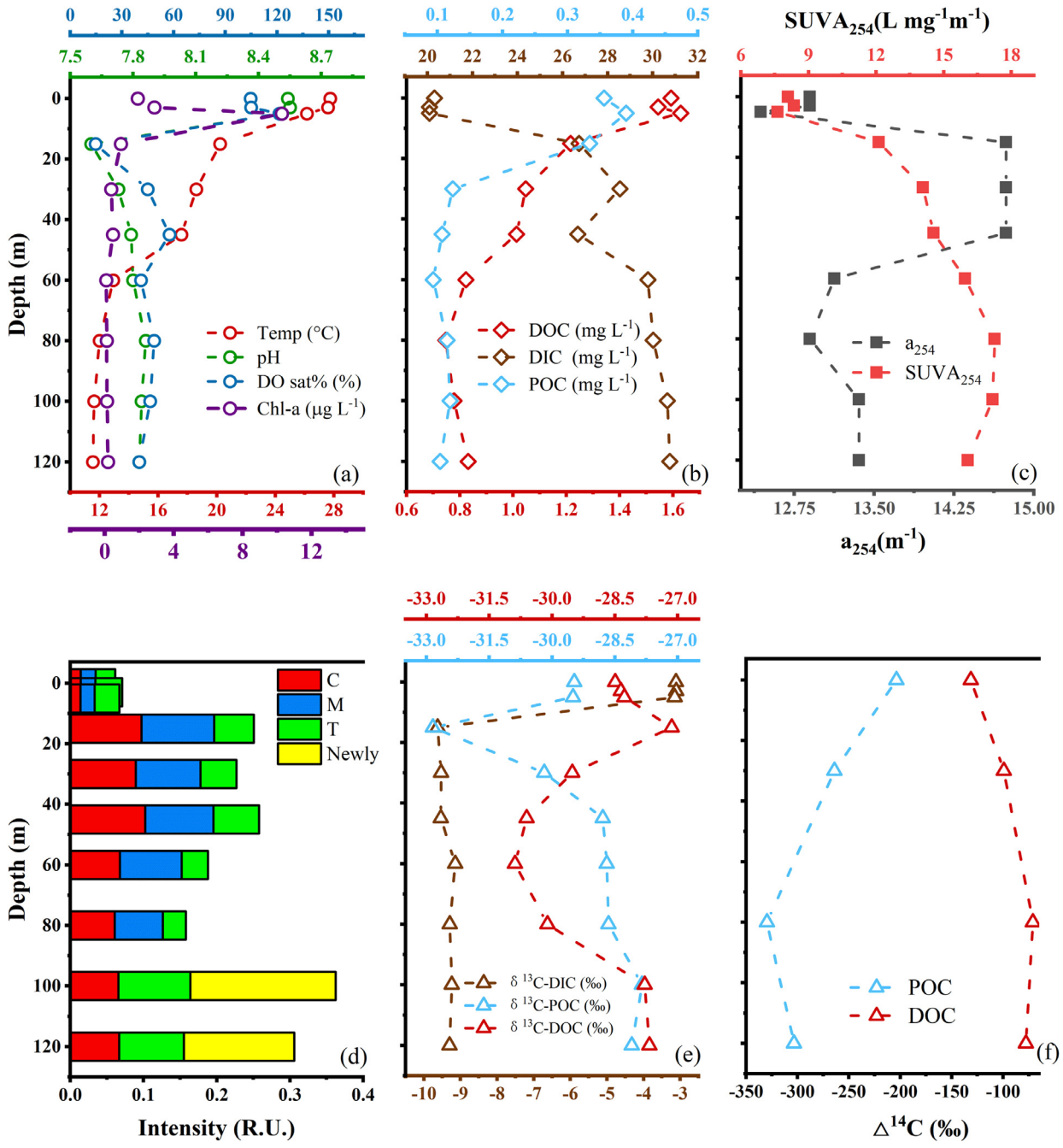


**Fig. 3.** Diagram of the changes of different parameters in the reservoir profile: a) The temperature, pH, chlorophyll-a and dissolved oxygen; b) the concentrations of DOC, DIC and POC; c) variation of $a_{254}$ and $SUVA_{254}$; d) the variations of different FDOM components (Peak C, M, T and Newly); e) the $\delta^{13}C$ values of POC and DOC; f) changes in $\Delta^{14}C_{DOC}$ and $\Delta^{14}C_{POC}$.

## 4. Discussion

### *4.1. Sources and transformation of organic carbon along the flow path*

A typical reservoir effect on POC is the removal of terrestrial OM from the water column and the increase in phytoplankton-derived OM due to the decrease in flow velocity, settling of suspended particles and reduction in water turbidity, thus increasing primary production (Matzinger et al., 2007). A continuous decrease in TSM was observed along the transition-reservoir transect (Fig. 2(b)), reflecting the effect of reservoirs in trapping terrestrial suspended particles and OM.

Phytoplankton mainly consumes water-soluble $CO_2$ for photosynthesis (Liu et al., 2018), which causes a reduction in the DIC concentration and an enrichment in $\delta^{13}C_{DIC}$ (Wang et al., 2019). The DIC concentration in the river area was approximately 30 mg $L^{-1}$, which is a typical value observed in karst regions but is more than 5 times higher than that observed in non-karst areas (Shih, 2018). In the HJD reservoir, the DIC concentration decrease and $\delta^{13}C_{DIC}$ enrichment along the river-reservoir transect suggested an enhanced primary production due to dam construction. The POC% was nearly 30%, which is a typical value for phytoplankton (Airoldi and Cinelli, 1997), agreed with the increased contribution of *in situ* production.

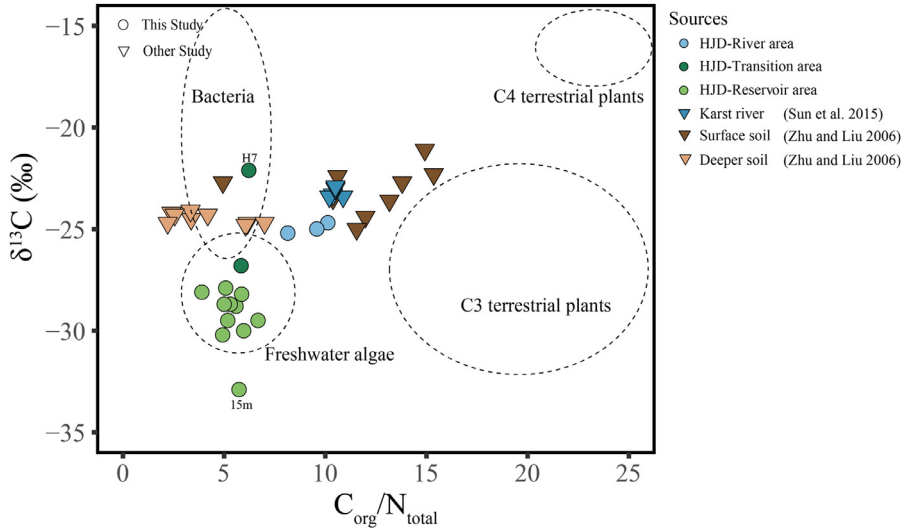


**Fig. 4.** Value of $\delta^{13}C$ and C/N ratio of POC in the HJD river - reservoir systems and end-members nearby the study area, including POC in karst river (Sun et al., 2015) and different depth karst soil (Zhu and Liu, 2006).

The values and ranges of $\delta^{13}C_{POC}$ (-30.0‰ to -24.7‰) as well as of the C/N weight ratio (6.0–10.1) further revealed a gradual transition from the soil OM observed in the river area to the typical phytoplankton source in the transition- reservoir area (Fig. 4) (Lamb et al., 2006). The soil OM source in the river area is likely an aged deep soil layer, as reflected by the depleted $\Delta^{14}C_{POC}$ (-550‰) value (Marwick et al., 2015). The changes in $\delta^{13}C_{POC}$ suggested that the newly produced POC had a more enriched $\delta^{13}C$ in the transition region than that in the reservoir. Earlier study in the Greifen Lake found that $\delta^{13}C_{POC}$ of phytoplankton-derived OC was much enriched during higher productivity season, and was attributed to the different carbon sources utilized ($CO_2$(aq) *vs*. bicarbonate) (Hollander and Mckenzie, 1991). The enriched $\delta^{13}C_{POC}$ in the transition region than that in the reservoir was also in accord with the higher productivity (see discussion in Section 4.3). Interestingly, the $\Delta^{14}C_{POC}$ value of the surface water in the transition reservoir region was more depleted than the "fresh" phytoplankton signal observed in the other regions (Chen et al., 2018), which could be caused by the depleted $\Delta^{14}C_{DIC}$ in karst areas (Liu et al., 2017). Therefore, the changes in the POC properties all reflect a typical reservoir effect on the POC sources in this head reservoir.

DOC in the river region indicated a much younger $\Delta^{14}C$ signal (-67±9‰) than did POC (Fig. 3(f)), which suggests that the contribution of the main source was derived from the surface soil (Fig. 5). Younger DOC than the POC were also observed in other rivers, which were attributed to the pre-aging process of POC in soil and the leaching of freshly produced OM (Raymond and Bauer, 2001b). The $SUVA_{254}$ (~15 L $mg^{-1}$ $m^{-1}$) values in the river area were much higher than those observed for the phytoplankton-derived DOM and even higher than the riverine DOM ranges observed during flooding (mainly soil-derived OM) (Fellman et al., 2013), suggesting the dominance of soil-derived OM, consistent with the information retrieved from $\Delta^{14}C_{DOC}$.

The increase in the DOC concentration (Fig. 2(b)) in the transition reservoir areas suggested a net addition of DOC in the water column, which is unlikely caused by the input from tributaries since DOC concentrations were similar between those tributaries (Table S2) and mainstream. The slight enrichment in $\delta^{13}C_{DOC}$ agreed with the enrichment in $\delta^{13}C_{POC}$ (Fig. 2(e)), suggesting that the DOC increase had a similar source to that of POC, *i.e., in situ* production. The decrease in $\Delta^{14}C_{DOC}$ in the transition reservoir areas was also consistent with the addition of $^{14}C$-depleted phytoplankton-derived OC (Fig. 2(f)). Aquatic primary production usually yields much lower $a_{254}$ and $SUVA_{254}$ values than do higher plants (Liu et al., 2019), which may have led to the low $SUVA_{254}$ value in the transition and reservoir areas by mixing with riverine DOM. He et al., (2020) also found a decrease in $SUVA_{254}$ with increasing autochthonous DOM in the Three Gorges Reservoir. Nevertheless, the decrease in $a_{254}$ and fluorescence intensity of each component in the transition reservoir areas implied that in addition to the input from *in situ* production, notable net removal of CDOM occurred (Fig. 2(c and d)). Photodegradation, microbial degradation and sorption by particles may all remove CDOM from the water column (Hansen et al., 2016). Due to the preferential utilization of non-aromatic OM, microbial degradation of DOM normally induces an increase in $SUVA_{254}$ (Hansen et al., 2016). Photodegradation is the likely mechanism, as it preferentially removes aromatic DOM, which is mainly of terrestrial origin, and causes a strong decrease in $a_{254}$ and $SUVA_{254,}$ as previously observed (He et al., 2020; Stubbins et al., 2010). The role of DOM sorption by sinking particles in the transition region remains unclear and merits further study.

The DOC characteristics (concentration, carbon isotopes, $SUVA_{254}$, $a_{254}$ and fluorescence intensity of each component) of the outlet samples were similar to those of the river samples, suggesting little transformation of the released water, which is related to the layer of the outlet (please refer to the discussion below).

### *4.2. Sources and transformation of organic carbon in the reservoir profile*

As water flows into the reservoir, due to changes in the physical conditions at the different depths, the biogeochemical processes may exhibit large differences down the profile, especially during the summer season, when notable thermal stratification occurs (Fig. 3(a)). Based on the physiochemical parameters, the reservoir profile was divided into four layers: surface layer (0–15 m), subsurface layer (15–45 m), intermediate layer (45–80 m) and bottom layer (80–120 m).

In the surface layer, the notably high DO% and POC% values, low DIC concentration, high DOC level and $\delta^{13}C_{DIC}$ enrichment all indicated substantial photosynthesis, thus producing and accumulating OC. In addition, the lowest $a_{254}$ and $SUVA_{254}$ values and fluores-

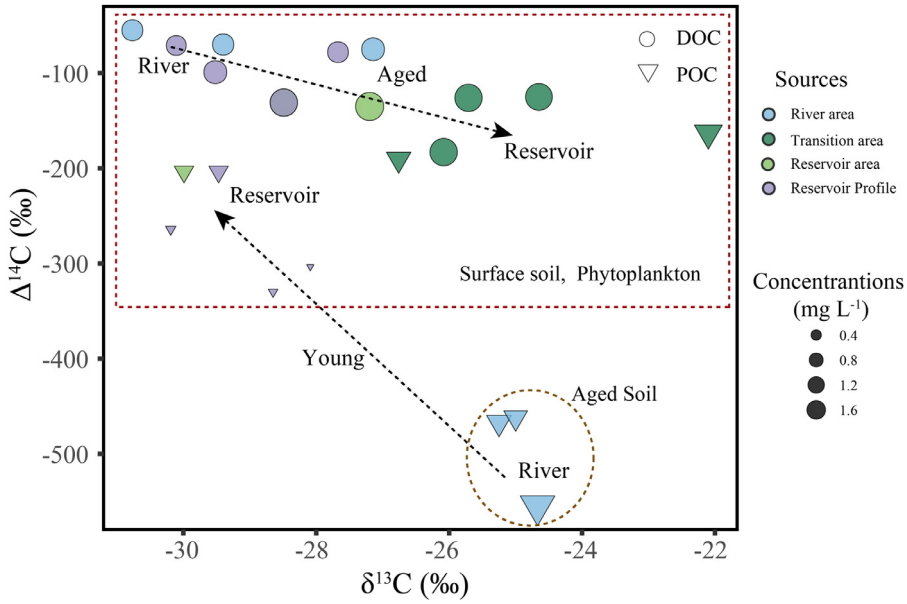


**Fig. 5.** Delineation of the major relationship of the OC in river-reservoir systems with the use of $\delta^{13}C$ and $\Delta^{14}C$ and major sources according to previous reports (Marwick et al., 2015).

cence intensity indicated the notable removal of CDOM by photochemical degradation (Hansen et al., 2016), as observed in the whole surface layer in the transition reservoir area. Sorption was unlikely an important process within the reservoir since most mineral particles had already settled in the transition region, as indicated by the changes in TSM (Fig. 2(b)). Therefore, this layer can be denoted as the production-photodegradation dominant layer (PPDL).

In the subsurface layer, a sharp decline in DO% at 15 m indicated a decrease in production and an increase in oxygen consumption. DIC and DOC at 15 m were still 2 mg $L^{-1}$ lower and 0.3 mg $L^{-1}$ higher, respectively, than those observed at the riverine site, suggesting that primary production still occurred at 15 m but much lower than that in the surface layer. An earlier study suggested that light still reached this layer (Hemsley et al., 2015); hence, a weaker BCP process could still occur. The lowest DO% and pH values at 15 m suggested notable OC mineralization. The sharp increases in $a_{254}$, $SUVA_{254}$, fluorescence intensity and $\delta^{13}C_{DOC}$ at 15 m were all consistent with microbial degradation/transformation (Romera-Castillo et al., 2011). The most depleted $\delta^{13}C_{POC}$ at 15 m was also in consist with weak primary production that utilized the depleted $\delta^{13}C_{DIC}$ in this layer. However, the POC concentration was largely decreased, suggesting that even there was primary production, it was very weak. Then the fraction of terrestrial POC could not be ignored in this layer. The enrichment in $\delta^{13}C_{POC}$ and depletion in $\Delta^{14}C_{POC}$ was also in accord with the increased fraction of terrestrial POC that were still suspended. Increases in the fraction of terrestrial OC could also explain the variation trend of $\delta^{13}C_{DOC}$ and $\Delta^{14}C_{DOC}$. Overall, this layer is denoted as the biodegradation dominant layer (BDL).

In the intermediate layer (45–80 m), since no light reached this layer, primary production and photodegradation were all negligible. All DIC and DOM parameters all resembled those at the riverine sites (Fig. 2 and Fig. 3), suggesting little transformation of carbon in this layer. The DOC characteristics of the released water were also similar to those of this layer since the water was released at a certain depth within this layer. Therefore, the effect of the dam on water release also depended on the outlet of the reservoir. The notably low POC concentration in this layer largely occurred due to the gradual removal of suspended particles during transport from the river to the reservoir. The $\Delta^{14}C_{DOC}$ and $\Delta^{14}C_{POC}$ continue to enrich and deplete, respectively, and was consisting with the increased fraction of terrestrial OM. Hence, this layer can be denoted as the river-mixing dominant layer (RMDL).

In the bottom layer (80–120 m), very interestingly, an obvious increase in $\delta^{13}C_{DOC}$ and $\delta^{13}C_{POC}$ along with a new FDOM component were occurred at 80 m. An earlier study indicated that due to the preferential utilization of the $^{13}C$ light component, an enrichment in $\delta^{13}C_{DOC}$ could be observed during microbial degradation (Meckenstock et al., 2004). The changes in the DOC isotopes and FDOM components were consistent with the microbial transformation of DOM observed in various aquatic environments (Jiao et al., 2010). An earlier study in lake overlying water also reported a similar phenomenon (Yang et al., 2014). The slight increase in DOC and $a_{254}$ in the bottom layer may be derived from diffusion from sediments. Therefore, this layer can be denoted as the anaerobic modification dominant layer (AMDL).

### *4.3. Quantifying the transformation of carbon among the different carbon pools and implications*

To quantitatively understand the transformation of carbon among the different carbon pools (DIC, POC and DOC), different parameters were applied. As mentioned above (Section 4.2), POC in the surface layer of the transition-reservoir area is predominantly of an autochthonous source, while the addition of DOC is also derived from *in situ* production. Therefore, the amount of OC contributed by *in situ* production ($OC_P$') can be estimated as the sum of POC concentration of the samples from the transition and reservoir areas ($POC_S$) and *in situ* production of DOC in the transition and reservoir areas ($DOC_P$), and a two-end member mixing model based on $\Delta^{14}C$ was applied to quantify the $DOC_P$ (Raymond and Bauer, 2001a) (see the supplementary text for a detailed analysis and calculation method; Table S3).

The results (Table S4) indicate that in the transition and reservoir areas, phytoplankton contributed ~50% to the total DOC, while this value decreased to < 5% in the RMDL and AMDL, suggesting that either the newly produced DOM was not largely transferred to the deeper layers or that the OM was largely degraded. In addition, although the CDOM experienced substantial photodegrada-

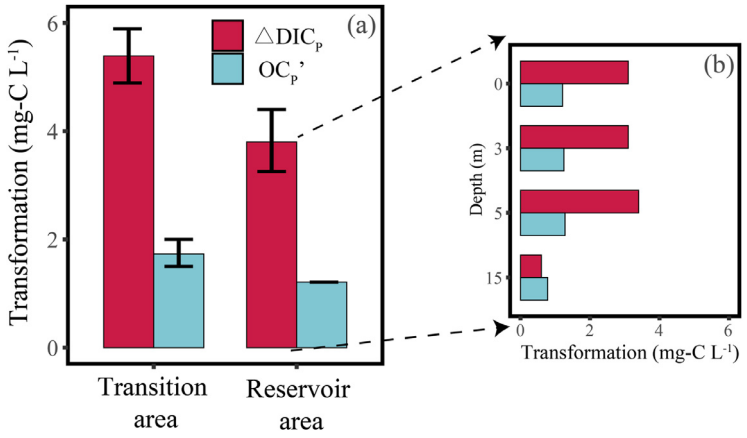


**Fig. 6.** Diagram of the amount of OC contributed by *in situ* production ($OC_P$') and DIC incorporated into the OM pool ($\Delta DIC_P$) in different regions: a) surface layer of transition-reservoir area; b) reservoir profile.

tion ($a_{254}$ and fluorescence intensity decreased by approximately 19% and 72%, respectively), only approximately 10% of the terrestrial DOM was removed (except at station H8). The unexpected high removal of terrestrial DOM at H8 was related to the relatively depleted $\Delta^{14}C_{DOC}$ value. We speculate that if this value is true (*i.e.*, no point contamination), it may then be related to the considerable sinking of suspended particles, which absorbed the terrestrial DOM.

The DIC concentration was mainly affected by photosynthesis, precipitation of carbonates and outgassing, which are modulated by various physiochemical conditions (Jan et al., 2010). Here, we define the difference between the sample ($DIC_S$) and riverine DIC values ($DIC_R$) as $\Delta DIC$. During the photosynthetic uptake of DIC by aquatic phototrophs, half of the DIC is bonded with $Ca^{2+}$ to form calcium carbonate (Liu et al., 2018), which is defined as $\Delta DIC_C$, and the other half is incorporated into the OM pool, which is defined as $\Delta DIC_P$ (Liu et al., 2018). In theory, $\Delta DIC_C = \Delta DIC_P$. In addition, the molar ratio of $\Delta DIC_C$ equals the molar of reduced $Ca^{2+}$ in BCP process. By considering the loss of DIC and $Ca^{2+}$ in different processes (BCP and carbonate precipitation due to changes in temperature), the transfer of DIC into the OC pool can be calculated (see supplementary file for detailed determination method and results).

The results indicated that $OC_P$' was much lower than $\Delta DIC_P$ (Fig. 6), which suggests two important facts: 1) a large amount of DIC was transferred to the OC pool in this karst area in summer ($\Delta DIC_P$ was ~3.1 to 6.3 mg $L^{-1}$ (15.5–31.5 mg-C $m^{-2}$ (10~21%), assuming similar carbon transfer occurred in the upper 5 m of the transition-reservoir area)), even higher than the riverine DIC concentration in non-karst areas (Shih, 2018); 2) only 20–24% remained in the OC pool in the water column with ~70% of the produced OC had an unknown fate in current study (Table S4). In most terrestrial ecosystems, aquatic primary production is limited by phosphorus (Wang, 2020). In the HJD, phosphate exhibited a sharp decrease from the river to the transition area and approached 0 mg $L^{-1}$ in the reservoir area (Table S2), suggesting that *in situ* production was also limited by P in our study area. The amount of autochthonous OC remaining in the water column was close to the P-bonded OC following the Redfield ratio, which ranged from approximately 1–1.3 mg $L^{-1}$ (supplementary Table S5). The much higher $\Delta DIC_P$ value may occur because P-containing OM was preferentially mineralized and re-entered the water column to support photosynthesis (Lomas et al., 2010); therefore, the reservoir acted as a factory that continuously converted DIC into OC, either preserved in sediments or emitted as $CO_2$. The OC burial efficiency is

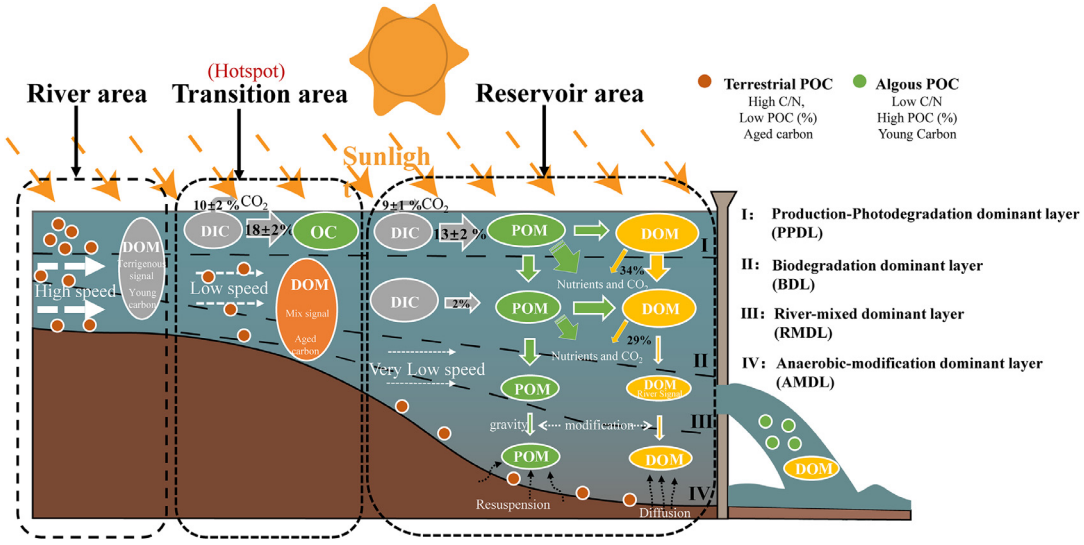


**Fig. 7.** Conceptual model of the effect of the reservoir on the modification of riverine organic matter and the processes of organic matter migration and transformation inside the reservoir.

therefore key to the global carbon budget. Earlier studies showed a highly variable OC burial efficiency (<10% to >90%) in other reservoirs (Mendonça et al., 2016). The low $pCO_2$ value in the transition and reservoir areas (Table S2) suggested that the OC produced through primary production may not be largely degraded. However, the net burial of OC in the HJD reservoir requires further research.

Interestingly, ΔDIC exhibited a higher value in the transition area than that in the reservoir area (Fig. 2(b), Table S5). Similar results were observed for $\Delta DIC_C$, which together implied that a higher primary production occurred in the transition area than that in the reservoir area (Liu et al., 2018), which could also be supported by the Chl-a data (Fig. 2(a)). The higher values of $\delta^{13}C_{DIC}$, DO%, DOC and POC in the transition area also revealed higher primary production, and were consistent with the observations in Greifen Lake that $\delta^{13}C_{DIC}$ and $\delta^{13}C_{POC}$ was more enriched during higher productivity season (Hollander and Mckenzie, 1991) (Fig. 2(a), (b) and (e)). We speculate that in the transition region, the high primary productivity might be related to the release of nutrients from terrestrial TSM (Wang et al., 2011). In contrast, the reservoir area mainly provided nutrients for the primary production process through OM degradation. These results emphasize the importance of the transition area in reservoir research. Previously, studies mainly focused on reservoir areas (Mendonça et al., 2016; Mendonca et al., 2017; Wang, 2020; Wang et al., 2019); however, our results reveal that transition areas are in fact hotspots for the primary production process and potential burial.

Furthermore, the results of our study also indicate that the reservoirs in karst areas exhibit a very high potential to affect the climate over non-karst areas under the condition of intensified human activities. Since *in situ* production is a nutrient-limited process, once nutrients enter the river system, the process is largely enhanced. Compared to non-karst areas, more sufficient DIC sources occur in karst areas to support this process, which promotes the burial of OC or degradation into $CO_2$ by a fast production-degradation process (Fig. 7). The net effect (degradation *vs*. preservation) may generate a high spatiotemporal variation regulated by physical conditions. Not only will a large amount of terrestrial OM be buried in reservoirs in the next ten to one hundred years, but a considerable DIC amount will also be converted into OM and be buried or degraded and emitted to the atmosphere.

## 5. Conclusion

Karst areas are carbon rich region, the effect of reservoir on carbon transport may have global significance, however, were not well constrained, especially the OC related biogeochemical processes. By applying multi-tracers, we found that during the transition from the river to the reservoir, terrestrial POC was replaced by an autochthonous source, along with the gradual removal of terrestrial DOC and net addition of autochthonous DOC (Fig. 7). Higher primary production was observed in the upper 5 m in the transition area (27±2.5 mg C $m^{-2}$ (18±2%)) than in the reservoir (19±3 mg C $m^{-2}$ (13±2%)), suggesting the transition area is in fact a hotspot for carbon transfer and should be given more attention in future studies. However, the results from current study couldn't represent the biogeochemical processes occurred throughout the year since there is only one systematic analysis in summer season.

The depth distribution of the DOC and POC concentrations and compositions during the stratification period revealed a structured carbon cycling pattern (Fig. 7). Higher production-degradation of OC occurred in the surface layer, while a lower *in situ* production but notable remineralization was observed in the subsurface layer. Little OC transformation occurred in the intermediate layer, and notable microbial transformation and/or sediment diffusion in the bottom layer (Fig. 7).

We further estimated that the amount of DIC (3.1–6.3 mg $L^{-1}$ (15.5–31.5 mg-C $m^{-2}$ (10–21%))) that was incorporated into OC pool caused by the reservoir was equal to/higher than the riverine DIC concentration in non-karst area, suggesting that the influence of reservoir on riverine carbon transport and transformation is more significant. Due to nutrient limitations and large amounts of available C, the reservoirs in karst regions are highly sensitive to anthropogenic activities, and would have a higher potential to affect the climate over non-karst areas.

## Authors' contributions

Yuanbi Yi performed all of the chemical analyses under the guidance of Siliang Li and Hongyan Bao; all of the authors designed the study, discussed the results and commented on the manuscript.

## Declaration of Competing Interest

The authors declare that they have no known competing financial interests or personal relationships that could have appeared to influence the work reported in this paper.

## Acknowledgements

This work was supported by the National Key R&D Programme of China (Grant No. 2016YFA0601002). Strategic Priority Research Program of Chinese Academy of Sciences (Grant No. XDB40000000). National Natural Science Foundation of China (Grant Nos. 41925002, 42076041). The authors are grateful to Wanfa Wang and Sainan Chen for their help during fieldwork.

## Supplementary materials

Supplementary material associated with this article can be found, in the online version, at doi:10.1016/j.watres.2021.116933.

## References

Airoldi, L., Cinelli, F., 1997. Sources and biochemical composition of suspended particulate material in a submarine cave with sulphur water springs. Mar. Biol. 128 (3), 537–545.
Bao, H., Wu, Y., Zhang, J., Deng, B., He, Q., 2014. Composition and flux of suspended organic matter in the middle and lower reaches of the Changjiang (Yangtze River) - impact of the Three Gorges Dam and the role of tributaries and channel erosion. Hydrol Process 28 (3), 1137–1147.
Beaulieu, E., Godderis, Y., Donnadieu, Y., Labat, D., Roelandt, C., 2012. High sensitivity of the continental-weathering carbon dioxide sink to future climate change. Nat Clim Chang 2 (5), 346–349.
Best, J., 2019. Author Correction: anthropogenic stresses on the world's big rivers. Nat Geosci.
Bushaw, K.L., Zepp, R.G., Tarr, M.A., Schulz-Jander, D., Bourbonniere, R.A., Hodson, R.E., Miller, W.L., Bronk, D.A., Moran, M.A., 1996. Photochemical release of biologically available nitrogen from aquatic dissolved organic matter. Nature 381 (6581), 404–407.
Chen, J., Yang, H., Zeng, Y., Guo, J., Song, Y., Ding, W., 2018. In: Combined Use of Radiocarbon and Stable Carbon Isotope to Constrain the Sources and Cycling of Particulate Organic Carbon in a Large Freshwater Lake, 625. China. Science of The Total Environment, pp. 27–38.
Cole, J.J., Prairie, Y.T., Caraco, N.F., McDowell, W.H., Tranvik, L.J., Striegl, R.G., Duarte, C.M., Kortelainen, P., Downing, J.A., Middelburg, J.J., 2007. Plumbing the global carbon cycle: integrating inland waters into the terrestrial carbon budget. Ecosystems 10 (1), 172–185.
Dams, W.C.o., 2000. Dams and Development: A New Framework for Decision-making: the Report of the World Commission on Dams. Earthscan.
Derrien, M., Brogi, S.R., Gonçalves-Araujo, R., 2019. Characterization of aquatic organic matter: assessment, perspectives and research priorities. Water Res. 163, 114908.
Dittmar, T., 2015. Reasons behind the long-term stability of dissolved organic matter. Biogeochemistry of Marine Dissolved Organic Matter 369–388 (Second Edition).
Fellman, J.B., Pettit, N.E., Kalic, J., Grierson, P.F., 2013. Influence of stream-floodplain biogeochemical linkages on aquatic foodweb structure along a gradient of stream size in a tropical catchment. Freshwater Science 32 (1), 217–229.

Griffin, C.G., Finlay, J.C., Brezonik, P.L., Olmanson, L., Hozaiski, R.M., 2018. Limitations on using CDOM as a proxy for DOC in temperate lakes. Water Res. 144, 719–727.
Grill, G., Lehner, B., Thieme, M., Geenen, B., Tickner, D., Antonelli, F., Babu, S., Borrelli, P., Cheng, L., Crochetiere, H., 2019. Mapping the world's free-flowing rivers. Nature 569 (7755), 215.
Gzqx (2018) Annual climate impact assessment of Guizhou province in 2018. Climate center of Guizhou province., Accessed date: 20 January 2019., http://gz.cma.gov.cn/.
Hansen, A.M., Kraus, T.E.C., Pellerin, B.A., Fleck, J.A., Downing, B.D., Bergamaschi, B.A, 2016. Optical properties of dissolved organic matter (DOM): effects of biological and photolytic degradation. Limnol. Oceanogr. 61 (3), 1015–1032.
He, D., Kai, W., Yu, P., Chen, H., Penghui, L., Yunyun, L., Shangbin, X., Quan, S., Yongge, S., 2020. Hydrological management constraints on the chemistry of dissolved organic matter in the Three Gorges Reservoir. Water Res. 116413 (0043–1354).
Hedges, J.I., 1992. Global biogeochemical cycles: progress and problems. Mar Chem 39 (1–3), 67–93.
Helms, J.R., Stubbins, A., Ritchie, J.D., Minor, E.C., Kieber, D.J., Mopper, K., 2008. Absorption spectral slopes and slope ratios as indicators of molecular weight, source, and photobleaching of chromophoric dissolved organic matter. Limnology & Oceanography 53 (3), 955–969.
Hemsley, V.S., Smyth, T.J., Martin, A.P., Frajka-Williams, E., Thompson, A.F., Damerell, G., Painter, S.C., 2015. Estimating Oceanic Primary Production Using Vertical Irradiance and Chlorophyll Profiles from Ocean Gliders in the North Atlantic. Environ. Sci. Technol. 49 (19), 11612–11621.
Holland, A., Stauber, J., Wood, C.M., Trenfield, M., Jolley, D.F., 2018. Dissolved organic matter signatures vary between naturally acidic, circumneutral and groundwater-fed freshwaters in Australia. Water Res., S0043135418301507.
Hollander, D.J., Mckenzie, J.A., 1991. CO2 control on carbon-isotope fractionation during aqueous photosynthesis: a paleo-pCO2 barometer. Geology 19 (9), 929–932.
IPCC Climate, C., 2007. The Physical Science Basis. Cambridge Univ. Press.
Jan, Åberg, Mats, JanssonAnders and Jonsson, 2010. Importance of water temperature and thermal stratification dynamics for temporal variation of surface water $CO_2$in a boreal lake. Journal of Geophysical Research Biogeosciences.
Jiao, N., Herndl, G.J., Hansell, D.A., Benner, R., Kattner, G., Wilhelm, S.W., Kirchman, D.L., Weinbauer, M.G., Luo, T., Chen, F., 2010. Microbial production of recalcitrant dissolved organic matter: long-term carbon storage in the global ocean. Nature Reviews Microbiology 8 (8), 593–599.
Lamb, A.L., Wilson, G.P., Leng, M.J., 2006. A review of coastal palaeoclimate and relative sea-level reconstructions using $\delta$13C and C/N ratios in organic material. Earth Science Reviews 75 (1–4), 29–57.
Leonard, A., Castle, S., Burr, G.S., Lange, T., Thomas, J., 2013. A Wet Oxidation Method for Ams Radiocarbon Analysis of Dissolved Organic Carbon in Water. Radiocarbon 55 (2–3), 545–552.
Liu, S., Feng, W., Song, F., Li, T., Guo, W., Wang, B., Wang, H., Wu, F., 2019. Photodegradation of algae and macrophyte-derived dissolved organic matter: a multi-method assessment of DOM transformation. Limnologica 77, 125683.
Liu, Z., Macpherson, G.L., Groves, C., Martin, J.B., Yuan, D., Zeng, S., 2018. Large and active CO 2 uptake by coupled carbonate weathering. Earth-Science Reviews 182, 42–49.
Liu, Z.H., Zhao, M., Sun, H.L., Yang, R., Chen, B., Yang, M.X., Zeng, Q.R., Zeng, H.T., 2017. Old" carbon entering the South China Sea from the carbonate-rich Pearl River Basin: coupled action of carbonate weathering and aquatic photosynthesis. Applied Geochemistry 78, 96–104.
Lomas, M.W., Burke, A.L., Lomas, D.A., Bell, D.W., Shen, C., Dyhrman, S.T., Ammerman, J.W., 2010. Sargasso Sea phosphorus biogeochemistry: an important role for dissolved organic phosphorus (DOP). Biogeosciences 6 (2) 7,2(2010-02-19).
Maavara, T., Lauerwald, R., Regnier, P., Van Cappellen, P., 2017. Global perturbation of organic carbon cycling by river damming. Nat Commun 8.
Marwick, T.R., Tamooh, F., Teodoru, C.R., Borges, A.V., Bouillon, S., 2015. The age of river-transported carbon: a global perspective. Global Biogeochem Cycles 29 (2), 122–137.
Matzinger, A., Pieters, R., Ashley, K.I., Lawrence, G.A., Wüest, A., 2007. Effects of impoundment on nutrient availability and productivity in lakes. Limnol. Oceanogr. 52 (6), 2629–2640.
Meckenstock, R.U., Morasch, B., Griebler, C., Richnow, H.H., 2004. Stable isotope fractionation analysis as a tool to monitor biodegradation in contaminated acquifers. J. Contam. Hydrol. 75 (3–4), 215–255.
Mendonça, R., Kosten, S., Sobek, S., Cardoso, S.J., Figueiredo-Barros, M.P., Estrada, C.H.D., Roland, F, 2016. Organic carbon burial efficiency in a subtropical hydroelectric reservoir. Biogeosciences 13 (11), 3331–3342.
Mendonca, R., Muller, R.A., Clow, D., Verpoorter, C., Raymond, P., Tranvik, L.J., Sobek, S., 2017. Organic carbon burial in global lakes and reservoirs. Nat Commun 8.
Mostofa, K.M.G., Jie, Y., Sakugawa, H., Liu, C.-Q, 2019. Equal Treatment of Different EEM Data on PARAFAC Modeling Produces Artifact Fluorescent Components That Have Misleading Biogeochemical Consequences. Environ. Sci. Technol..
Piao, S., Ciais, P., Huang, Y., Shen, Z., Peng, S., Li, J., Zhou, L., Liu, H., Ma, Y., Ding, Y., Friedlingstein, P., Liu, C., Tan, K., Yu, Y., Zhang, T., Fang, J., 2010. The impacts of climate change on water resources and agriculture in China. Nature 467 (7311), 43–51.
Raymond, P.A., Bauer, J.E., 2001a. DOC cycling in a temperate estuary: a mass balance approach using natural 14C and 13C isotopes. Limnology & Oceanography 46 (3), 655–667.
Raymond, P.A., Bauer, J.E., 2001b. Riverine export of aged terrestrial organic matter to the North Atlantic Ocean. Nature 409 (6819), 497–500.
Raymond, P.A., Spencer, R.G.M, 2015. Biogeochemistry of Marine Dissolved Organic Matter. Elsevier, pp. 509–533.
Romera-Castillo, C., Sarmento, H., Álvarez-Salgado, X.A., Gasol, J.M., Marrasé, C., 2011. Net Production and Consumption of Fluorescent Colored Dissolved Organic Matter by Natural Bacterial Assemblages Growing on Marine Phytoplankton Exudates. Appl. Environ. Microbiol. 77 (21), 7490–7498.
Shih, Y.-t., 2018. Dynamic responses of DOC and DIC transport to different flow regimes in a subtropical small mountainous river. Hydrology and Earth System Sciences 22, 6579–6590.
Stubbins, A., Spencer, R.G., Chen, H., Hatcher, P.G., Mopper, K., Hernes, P.J., Mwamba, V.L., Mangangu, A.M., Wabakanghanzi, J.N., Six, J., 2010. Illuminated darkness: molecular signatures of Congo River dissolved organic matter and its photochemical alteration as revealed by ultrahigh precision mass spectrometry. Limnol. Oceanogr. 55 (4), 1467–1477.
Stuiver, M., Polach, H.A., 1977. Discussion Reporting of 14C Data. Radiocarbon 19 (3), 355–363.
Sun, H., Han, J., Zhang, S., Lu, X., 2015. Carbon isotopic evidence for transformation of DIC to POC in the lower Xijiang River, SE China. Quaternary International 380-381 (SEP.4), 288–296.
Teeling, H., Fuchs, B.M., Becher, D., Klockow, C., Gardebrecht, A., Bennke, C.M., Kassabgy, M., Huang, S.X., Mann, A.J., Waldmann, J., Weber, M., Klindworth, A., Otto, A., Lange, J., Bernhardt, J., Reinsch, C., Hecker, M., Peplies, J., Bockelmann, F.D., Callies, U., Gerdts, G., Wichels, A., Wiltshire, K.H., Glockner, F.O., Schweder, T., Amann, R., 2012. Substrate-controlled succession of marine bacterioplankton populations induced by a phytoplankton bloom. Science 336 (6081), 608–611.
Telmer, K., Veizer, J., 1999. Carbon fluxes, pCO2 and substrate weathering in a large northern river basin, Canada: carbon isotope perspectives. Chem. Geol. 159 (1–4), 61–86.
Wang, F., 2020. Impact of a large sub-tropical reservoir on the cycling of nutrients in a river. Water Res. 186.
Wang, S., Qian, X., Han, B.-P., Wang, Q.-H., Ding, Z.-F., 2011. Physical limnology of a typical subtropical reservoir in south China. Lake Reserv Manag 27 (2), 149–161.
Wang, W.-F., Li, S.-L., Zhong, J., Maberly, S.C., Li, C., Wang, F.-S., Xiao, H.-Y., Liu, C.-Q., 2019. Climatic and anthropogenic regulation of carbon transport and transformation in a karst river-reservoir system. Science of The Total Environment, 135628.
Xu, X., Trumbore, S.E., Zheng, S., Southon, J.R., Mcduffee, K.E., Luttgen, M., Liu, J.C., 2007. Modifying a sealed tube zinc reduction method for preparation of AMS graphite targets: reducing background and attaining high precision. Nuclear Inst & Methods in Physics Research B 259 (1), 320–329.
Yang, L., Choi, J.H., Hur, J., 2014. Benthic flux of dissolved organic matter from lake sediment at different redox conditions and the possible effects of biogeochemical processes. Water Res. 61 (Complete), 97–107.
Zhong, J., Li, S.L., Ibarra, D.E., Ding, H., Liu, C.Q., 2020. Solute Production and Transport Processes in Chinese Monsoonal Rivers: implications for Global Climate Change. Global Biogeochem Cycles.
Zhou, Y., Guo, H., Lu, H., Mao, R., Zheng, H., Wang, J., 2015. Analytical methods and application of stable isotopes in dissolved organic carbon and inorganic carbon in groundwater. Rapid Communications in Mass Spectrometry 29 (19), 1827–1835.
Zhu, S., Liu, C., 2006. Vertical patterns of stable carbon isotope in soils and particle-size fractions of karst areas, Southwest China. Environmental Geology 50 (8), 1119–1127.